2021

Toward Resolving Disparate Accounts of the Extent and Magnitude of Nitrogen Fixation in the Eastern Tropical South Pacific Oxygen Deficient Zone

Corday R. Selden
Old Dominion University, cseld001@odu.edu

Margaret R. Mulholland
Old Dominion University, mmulholl@odu.edu

Brittany Widner
Old Dominion University, bwidn001@odu.edu

Peter Bernhardt
Old Dominion University, pbernhar@odu.edu

Amal Jayakumar

Original Publication Citation

Selden, C.R., Mulholland, M.R., Widner, B., Bernhardt, P. & Jayakumar, A. (2021). Toward resolving disparate accounts of the extent and magnitude of nitrogen fixation in the Eastern Tropical South Pacific oxygen deficient zone. *Limnology and Oceanography*, 66(5), 1950-1960. https://doi.org/10.1002/lno.11735

LIMNOLOGY and OCEANOGRAPHY

ASLO

Limnol. Oceanogr. 66, 2021, 1950–1960

doi: 10.1002/lno.11735

Toward resolving disparate accounts of the extent and magnitude of nitrogen fixation in the Eastern Tropical South Pacific oxygen deficient zone

Corday R. Selden,[1*] **Margaret R. Mulholland**,[1] **Brittany Widner**,[1,3] **Peter Bernhardt**,[1] **Amal Jayakumar**[2]

[1]Old Dominion University, Norfolk, Virginia
[2]Princeton University, Princeton, New Jersey
[3]Woods Hole Oceanographic Institute, Woods Hole, Massachusetts

Abstract

Examination of dinitrogen (N_2) fixation in the Eastern Tropical South Pacific oxygen deficient zone has raised questions about the range of diazotrophs in the deep sea and their quantitative importance as a source of new nitrogen globally. However, technical considerations in the deployment of stable isotopes in quantifying N_2 fixation rates have complicated interpretation of this research. Here, we report the findings of a comprehensive survey of N_2 fixation within, above and below the Eastern Tropical South Pacific oxygen deficient zone. N_2 fixation rates were measured using a robust ^{15}N tracer method (bubble removal) that accounts for the slow dissolution of N_2 gas and calculated using a conservative approach. N_2 fixation was only detected in a subset of samples (8 of 125 replicated measurements) collected within suboxic waters ($< 20\ \mu mol\ O_2\ kg^{-1}$) or at the oxycline. Most of these detectable rates were measured at nearshore stations, or where surface productivity was high. These findings support the hypothesis that low oxygen/high organic carbon conditions favor non-cyanobacterial diazotrophs. Nevertheless, this study indicates that N_2 fixation is neither widespread nor quantitatively important throughout this region.

Nitrogen (N) limits productivity across a vast expanse of the ocean's surface (Moore et al. 2013). Consequently, N availability plays an important role in regulating ocean carbon cycling and global climate (Falkowski 1997; Karl et al. 2002; Deutsch et al. 2004). Unlike other important macronutrients such as soluble reactive phosphorus (SRP), reactive N (N_r) has biological sources and sinks capable of modulating the N_r pool in response to environmental forcings. N_r losses occur primarily in anoxic sediments and pelagic oxygen deficient zones where nitrate (NO_3^-) respiration (denitrification) and anaerobic ammonium oxidation (anammox) are energetically favorable (Devol 2008). In contrast, the distribution and magnitude of oceanic dinitrogen (N_2) fixation, the prokaryote-mediated conversion of relatively unreactive N_2 gas to N_r, remain poorly constrained because diazotrophic groups are ecologically diverse and can be metabolically flexible (Zehr and Capone 2020).

The ocean's largest pelagic oxygen (O_2) deficient zones occur in the Eastern Tropical North and South Pacific Oceans. Together, these account for roughly one-quarter of marine N_r loss (DeVries et al. 2012). When denitrified waters surface, DIN is exhausted in advance of SRP, creating conditions thought to favor N_2 fixation (Deutsch et al. 2007; Weber and Deutsch 2014) because assimilation of ammonium and NO_3^-, the primary forms of DIN available in the ocean, are typically less energetically-costly means of acquiring N (Falkowski 1983). The degree to which N_r inputs and losses are spatially coupled is hypothesized to be a function of the availability of dissolved iron (Fe), a key cofactor in the N_2 fixation enzyme (Weber and Deutsch 2014; Bonnet et al. 2017). This mechanism is believed to play a major role in balancing the ocean's N_r inventory (e.g., Weber and Deutsch 2014).

Direct observations of N_2 fixation (e.g., Knapp et al. 2016; Knapp et al. 2018) suggest that N_r inputs and losses are relatively decoupled due to Fe limitation in the Eastern Tropical South Pacific (Dekaezemacker et al. 2013; Weber and Deutsch 2014; Kondo and Moffett 2015). Nevertheless, and despite significant concentrations of DIN ($> 1\ \mu M$), Eastern Tropical South Pacific waters harbor a diverse assemblage of

*Correspondence: cseld001@odu.edu

Additional Supporting Information may be found in the online version of this article.

predominantly non-cyanobacterial diazotrophs (Fernandez et al. 2011; Bonnet et al. 2013; Löscher et al. 2014; Chang et al. 2019) reported to actively fix N_2 at low, but persistent, rates throughout the water column (e.g., Fernandez et al. 2011; Bonnet et al. 2013). If this pattern held true throughout the ocean's interior, it would mean that sub-euphotic diazotrophs contribute a significant fraction (~ 6–32%) of the ocean's N_r inputs (Benavides et al. 2018). Moreover, the widespread occurrence of N_2 fixation under DIN-replete conditions would suggest that new N_r inputs (via diazotrophy) are either less sensitive (*see* discussion in Bombar et al. 2016) to changes in the N_r inventory (via denitrification/anammox) than hypothesized (e.g., Weber and Deutsch 2014), or that our conception of the feedback process between them is incomplete.

Interpretation of N_2 fixation rate data from the Eastern Tropical South Pacific and other mesopelagic systems has, however, been hampered by methodological issues associated with implementation of the $^{15}N_2$ tracer incubation approach (Montoya et al. 1996) where diazotroph activity is low (*see* discussion in White et al. 2020). Using a more conservative approach to quantifying N_2 fixation rates, we present a comprehensive examination of measurements from the Eastern Tropical South Pacific within the context of past work.

Methods

Hydrographic data and sample collection

Samples were collected in January 2015, while aboard the R/V *Atlantis*. Vertical profiles of temperature, salinity, photosynthetically-active radiation, dissolved O_2, and chlorophyll *a* fluorescence were obtained using a Sea-Bird SBE 11plus conductivity-temperature-depth (CTD) sensor package equipped with a model 43 dissolved O_2 sensor, a QSP200L Biospherical photosynthetically-active radiation sensor, and a WET Labs ECO-AFL chlorophyll *a* fluorometer. Samples for nutrient analysis were collected from Niskin bottles affixed to the CTD rosette and, within the O_2 deficient zone, from a pump profiling system. Samples for NO_3^- plus nitrite (NO_2^-) and SRP were syringe-filtered through a Sterivex filter (0.2 μm). Filtrate was collected and stored upright in acid-washed polyethylene bottles at – 20°C until analysis at Old Dominion University using an Astoria-Pacific autoanalyzer and standard colorimetric protocols (Parsons et al. 1984). NO_2^- samples were filtered by gravity through a 0.2 μm Millipore filter directly from the Niskin bottles into acid-washed Falcon tubes. These samples were analyzed immediately using a manual colorimetric method on a Shimadzu (UV-1800) spectrophotometer (Pai et al. 1990). The detection limits for NO_2^-, $NO_3^- + NO_2^-$, and SRP analyses were 0.02, 0.14, and 0.03 μM (3σ, n = 7), respectively.

Oxic water samples for N_2 fixation incubations and particulate N (PN) enrichment and mass were collected in 10 L carboys from Niskin bottles mounted to the CTD rosette. Incubations from the shallow oxic zone were conducted in clear, 1.2 L PETG bottles in triplicate. Duplicate water samples were also filtered at the initial time point onto pre-combusted (450°C, 2 h) 0.3 μm glass fiber filters (GF-75, Advantec MFS, Dublin, CA) to measure particulate carbon and PN concentrations and initial PN ^{15}N enrichment. These samples were frozen and stored at – 20°C until analysis at Old Dominion University (*see* below).

Incubation samples from below the suboxic layer were collected in triplicate directly from Niskin bottles into 4.3 L amber glass bottles. Particulate carbon/PN samples were collected as described above. Within the suboxic layer, samples were pumped directly from depth into He-flushed 4.3 L amber glass bottles using a submersible water pump affixed to a small CTD as described by Selden et al. (2019). To limit O_2 contamination, bottles were first filled with sample then submerged in a ~ 50 L tub of O_2 deficient water. Sample bottles were flushed continuously from the bottom to avoid back-flow from the tub until they had been filled three times over. With this set-up, a roughly 0.5 m thick layer of continuously replenished low-O_2 water covered the bottles as they flushed, preventing atmospheric O_2 contamination and maintaining in situ temperature as samples were collected.

N_2 fixation rate measurements

Incubation set-up

N_2 fixation rates were determined using the bubble removal technique (e.g., Jayakumar et al. 2017), a modified version of the $^{15}N_2$ incubation-based assay of Montoya et al. (1996) that accounts for the slow dissolution time of N_2 gas (Mohr et al. 2010). In brief, approximately 1 or 4 mL additions (to 1.2 and 4.3 L incubation bottles, respectively) of pressurized, highly enriched (~ 99%, Cambridge Isotopes, Tewksbury MA) $^{15}N_2$ was added to PETG or glass incubation bottles. Prior to these additions, incubation bottles were filled completely and any air bubbles were removed. Additions were made using a gas-tight syringe (VICI Valco Instruments, Houston, TX) through a silicon septa cap that allowed for small changes in volume. Sample bottles were gently inverted for 15 min using a seesaw, as described by Selden et al. (2019), to increase the rate of gas dissolution. After mixing, the remaining gas bubble was removed using a syringe so that the $^{15}N_2$ enrichment of the seawater remained constant throughout the incubation period. Sample bottles were then incubated under approximate in situ light and temperature conditions.

For euphotic zone samples, incubation bottles were placed in on-deck incubators that were continuously flushed with surface seawater to maintain temperature. Appropriate light conditions, as determined using the CTD-mounted photosynthetically-active radiation sensor, were approximated using neutral-density screens. Samples collected below the euphotic zone were maintained in the dark, either in a walk-in cold van (~ 12°C) or refrigerator (~ 4°C), whichever more closely simulated ambient environmental conditions at the

depths samples were collected. For samples collected below the suboxic zone, incubation bottles were placed in a dark, walk-in refrigerator (~ 4°C), where they were incubated for ~ 48 h. All other samples were incubated for ~ 24 h.

Contamination (^{15}N-labeled DIN) has been previously been reported for some commercially available $^{15}N_2$ stocks (Dabundo et al. 2014; White et al. 2020). While the purity of the tracer stocks used here were not directly tested, we note that this issue has never been reported for $^{15}N_2$ gas from Cambridge Isotope Laboratories. Additionally, after 24 and 48 h incubations, generally little ^{15}N enrichment was detected in the particulate N pool (i.e., rates of N_2 fixation were largely undetectable, *see* Results and Discussion). It is thus highly unlikely that our stocks were contaminated.

At the end of the incubation, aliquots (6 mL) were transferred to He-flushed 12 mL Exetainers™ using a gas-tight syringe (Hamilton 1000 series, Reno, NV) to determine the ^{15}N enrichment of the N_2 pool To these samples, 50 μL of 50% w/v $ZnCl_2$ (Thermo Fisher Scientific, Waltham, MA) was added to ensure the termination of microbial activity. The remaining sample was immediately filtered on 0.3 μm glass fiber filters (GF-75, Advantec MFS Inc, Dublin, CA). Filters were frozen and stored in sterile microcentrifuge tubes at − 20°C until analysis at Old Dominion University. Exetainer samples were stored at room temperature until analysis at Princeton University. They did not undergo any significant pressure changes (e.g., from air shipping) during storage.

Sample analysis

$^{15}N_2$ gas samples were analyzed at Princeton University using a Europa 20–20 isotope ratio mass spectrometer (IRMS), following Jayakumar et al. (2017). $^{15}N_2$ enrichment in sample incubations ranged from 2.22 to 8.57 atom-% (mean = 3.64 ± 0.04 atom-%, n = 159). Particulate samples, collected both from the environment (t = 0) and from incubation bottles (t = f), were dried (50°C for ~ 2 d) and then pelletized in tin discs at Old Dominion University. ^{15}N enrichment of the PN pool and its mass were subsequently determined using a Europa 20–20 IRMS equipped with an automated N and carbon analyzer. Samples from initial (non-enriched) and final (potentially ^{15}N tracer-enriched) time points were pelletized separately, stored in separate desiccators, and analyzed separately to avoid carry-over contamination.

The detection limit for PN mass was calculated separately for each run using 12.5 μg N ammonium sulfate standards (IA-RO45, SerCon, Cheshire, UK; 3σ, n = 7), which were calibrated using standards from the National Institute of Standards and Technology. The mean detection limit among natural abundance instrument runs (n = 8) in this study was 2.06 μg N. Since the accuracy of enrichment analysis diminishes at lower mass (White et al. 2020) and low N_2 fixation rates are sensitive to small variations in ^{15}N enrichment, we assumed a conservative lower linearity limit of 10 μg N based on instrument performance during the time samples were analyzed (Suppl. Fig. 1). This value is consistent with current "best practice" recommendations from the scientific community (White et al. 2020). If sample mass was below 10 μg N, ^{15}N enrichment data from that sample was discarded. A standard curve (1.17–100 μg N) was also run each day to verify measurement linearity.

N_2 fixation rate calculations

N_2 fixation rates were calculated as described by Montoya et al. (1996):

$$\mathrm{NFR} = \frac{A_{PN_{t=f}} - A_{PN_{t=0}}}{A_{N_2} - A_{PN_{t=0}}} \times \frac{[\bar{PN}]}{\Delta t} \quad (1)$$

where $A_{PN_{t=f}}$, $A_{PN_{t=0}}$, and A_{N_2} represent the atom-% ^{15}N enrichment of the final and initial PN pool, and the incubation's N_2 pool, respectively. Incubation duration is denoted as Δt; $[\bar{PN}]$ is the mean concentration of PN across the incubation period. If a t = 0 measurement was not available from the exact location of the incubation water, then the final PN concentration and the mean $A_{PN_{t=0}}$ within either oxic or suboxic waters (whichever was appropriate) were used in the calculation in place of the $[\bar{PN}]$ and direct $A_{PN_{t=0}}$ measurement.

N_2 fixation was considered detectable if $\left(A_{PN_{t=f}} - A_{PN_{t=0}}\right)$ was greater than three times the standard deviation of seven 12.5 μg standards run daily with enriched ($A_{PN_{t=f}}$) samples (Ripp 1996). To calculate minimum detectable rates i.e., detection limits, this minimum detectable enrichment value (mean = 0.0054 ± 0.0026 atom-% across 11 IRMS runs) was substituted for $\left(A_{PN_{t=f}} - A_{PN_{t=0}}\right)$ in Eq. 1 (Jayakumar et al. 2017; White et al. 2020). Consequently, detection limits scale with PN concentration. In this study, the mean and median detection limit for N_2 fixation rates were 3.00 and 1.09 nmol N L^{-1} d^{-1}, respectively. All requisite information for calculating rates for each incubation is available on BCO-DMO (http://www.bco-dmo.org/project/742492).

N_2 fixation rates were considered detectable at a given location if ^{15}N enrichment was detected in at least two replicate incubations. Where two replicates were deemed detectable but the third was not, a mean N_2 fixation rate was calculated by forcing the undetectable rate to zero (Bonnet et al. 2013; Chang et al. 2019). Rate error was assessed by taking the standard deviation of rates from replicate incubations (Suppl. Text 1). These values are provided in Suppl. Table 1 alongside associated hydrographic data. To ensure that detectable changes in $A_{PN_{t=f}}$ were due to diazotrophy, control incubations were conducted at a subset of stations (Suppl. Text 2; Suppl. Table 2).

Results and discussion

Regional hydrography

Our study area encompassed both offshore and nearshore waters. Upwelling, visible as a decrease in sea surface temperature (Fig. 1A), was apparent near the Peruvian coast during the

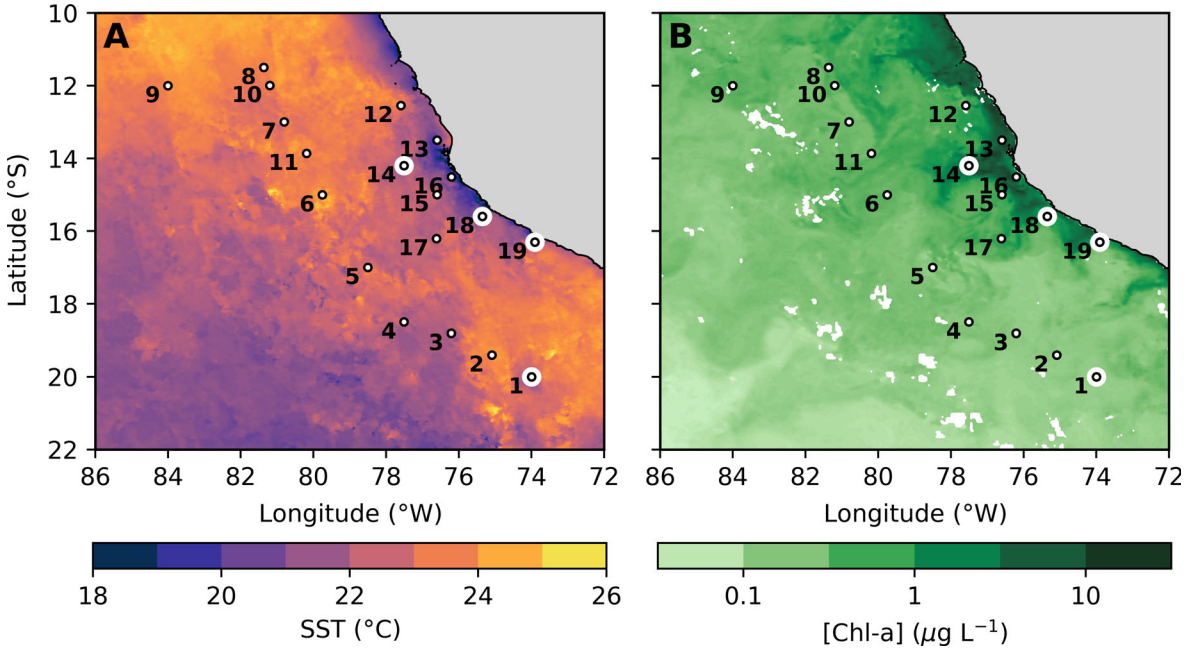

Fig. 1. Mean MODIS (NASA Goddard Space Flight Center 2018 Reprocessing) sea surface temperature (SST; **A**) and chlorophyll *a* concentration ([Chl-a]; **B**) for January 2015 overlain by stations. Large white dots indicate locations where N_2 fixation was detected.

study period (January 2015). These cooler waters were associated with elevated surface chlorophyll *a* (Fig. 1B) and high surface nutrient concentrations. At the shallowest (< 750 m depth) and most nearshore stations, the concentrations of DIN and SRP exceeded 14 and 1 μM, respectively, in the upper 10 m (Sta. 13, 16 and 19; Suppl. Fig. 2A,B). Surface DIN and SRP concentrations were slightly lower at other nearshore stations (Sta. 12, 14, 15, and 18), and decreased to < 4 and < 0.7 μM, respectively, at most offshore stations. In addition to transporting macronutrients, upwelling can supply surface waters with Fe and other trace elements liberated from shelf sediments, provided that upwelled waters remain relatively reducing (Rapp et al. 2020).

Suboxia (< 20 μmol O_2 kg^{-1}) was detected at all stations. The suboxic layer shoaled to an average depth of 80 m among nearshore stations (12–19; Suppl. Fig. 2D). Here, the thermocline was shallower and stronger (Suppl. Fig. 2E). At offshore stations to the south (> 16.5°S, Sta. 1–5), the suboxic layer was generally thinner particularly at Sta. 4 and 5, the latter of which was atop the Nazca Ridge. The average suboxic layer thickness at the southern stations was 360 m compared to averages of 640 and 540 m among northern offshore (< 16.5°S, Sta. 6–11) and nearshore stations, respectively. Functionally anoxic conditions were observed in the upper suboxic layer at all stations except Sta. 5, as indicated by NO_2^- concentrations in excess of 0.5 μM (Thamdrup et al. 2012). For offshore stations (Sta. 1–11), these conditions occurred between ~ 100 and 380 m depth.

Regional distribution of N_2 fixation

We assessed N_2 fixation rates in 61 samples collected within the oxic (> 20 μmol kg^{-1} O_2), euphotic waters, 59 samples collected within suboxic waters, and five samples collected in oxic waters beneath the O_2 deficient zone. Of these, N_2 fixation was detected in only eight samples (Figs. 1, 2, Suppl. Table 1), five from two stations at the southern end of our study site (Sta. 18 and 19, 5 depths), one from a particularly productive site (depth-integrated chlorophyll *a*: 36.7 mg m^{-2}, particulate C: 20–65 μM) slightly offshore (Sta. 14, 1 depth), and two from an offshore site (Sta. 1). Where detectable, N_2 fixation rates were low (0.18 ± 0.13–0.77 ± 0.003 nmol N L^{-1} d^{-1}; Suppl. Table 1). By applying a conservative limit of quantification (Selden et al. 2019), calculated by propagating a minimum quantifiable change in A_{PN} (10σ, n = 7 12.5 μg standards; Ripp 1996) through Eq. 1, we assert that even the detectable N_2 fixation rates reported here cannot be accurately quantified. The quantification limits where N_2 fixation was detected ranged from 0.4 to 1.4 nmol N L^{-1} d^{-1} (Suppl. Table 1), representing an upper bound on N_2 fixation rates. In contrast, detection limits, i.e., the lower bounds for these rate measurements, ranged from 0.09 to 0.3 nmol N L^{-1} d^{-1} (Suppl. Table 1).

The role of dissolved oxygen

Seven of the eight locations (of 125 total) where N_2 fixation was detected were within suboxic waters. At all but one of these (Sta. 18, 100 m), NO_2^- concentrations exceeded 0.5 μM, suggesting functional anoxia (Thamdrup et al. 2012). The

Table 1. Volumetric N_2 fixation rates (NFRs) reported from the Eastern Tropical South Pacific oxygen deficient zone (ODZ) and neighboring waters.*

Reference	Date	Oceanic Niño Index†	Depth range	Mean NFR or range (nmol N L^{-1} d^{-1})‡	Sample collection	Method§	Filter size	Incub. vol. (L)	Min. filter mass (μg N)	Min. detectable enrichment	$A_{PN_{t=0}}$¶ measured directly?
Fernandez et al. 2011	Oct/ Nov 2005	−0.3	Surface Upper oxycline	0.89±0.08 (*n*=17) 0.075±0.07 (*n*=8)	Niskin**	TBM	0.7 GF/F	2	Not reported††	Not reported	Not reported
	Feb 2007	0.7	Surface Upper oxycline Upper ODZ (<400 m)	0.66±0.7 (*n*=10) 1.71±1.03 (*n*=17) 1.27±1.2 (*n*=13)							
Bonnet et al. 2013	Feb/ Mar 2010	1.3	Surface – 2000 m	BDL – 0.80 (*n*=40)	Niskin‡‡	TBM§§	0.7 GF/F	4.5	3.8¶¶	0.0005 atom-%, (3σ, *n*=10 IAEA reference samples)	No***
	Mar/ Apr 2011	−0.8	Surface – 2000 m Below ODZ (400–2000 m)	BDL – 0.26±0.12 (*n*=216) 0.00±0.01–0.21±0.13							Yes
Dekaezemacker et al. 2013	Feb/ Mar 2010	1.3	Surface – 200 m	<0.06–0.88	Niskin‡‡	TBM§§	0.7 GF/F	4.5	2.9¶¶	0.0005 atom-%, (3σ, *n*=10 IAEA reference samples)	Surface only
	Mar/ Apr 2011	−0.8	Surface – 200 m	BDL – 0.87							Yes
Löscher et al. 2014	Jan/ Feb 2009	−0.8	Surface Oxycline to ODZ (~40–350 m)	<24.8±8.4 <0.4	Niskin Pump‡‡	TBM	0.7 GF/F	2	~3†††	Not reported	Yes
Knapp et al. 2016	Feb/ Mar 2010	1.3	Surface – 180 m	0.25±0.11–0.54±0.72‡‡‡	Niskin	TBM	0.7 GF/F	4	10	Not reported§§§	Yes¶¶¶
	Mar/ Apr 2011	−0.8	Surface – 150 m	0.15±0.16–0.41±0.15‡‡‡							
Löscher et al. 2016	Nov/ Dec 2012	0.0	Surface ODZ	2.2±3.6 0.5±1.36	Niskin or pump	ESM****	0.7 GF/F	4.5	3.9	0.0005 atom-%	Yes

(Continues)

Table 1. Continued

Reference	Date	Oceanic Niño Index[†]	Depth range	Mean NFR or range (nmol N L^{-1} d^{-1})[‡]	Sample collection	Method[§]	Filter size	Incub. vol. (L)	Min. filter mass (μg N)	Min. detectable enrichment	$A_{PN_{t=0}}$[¶] measured directly?
			Below ODZ	0.18±0.28							
Chang et al. 2019	Jul 2011	−0.4	Euphotic zone	BDL – 3.9	Niskin**	BRM	0.7 GF/F	2.5	2	0.0025 (3σ, *n*=7 12 μg N standards)	Yes
			Upper ODZ (<400 m)	BDL				5			
This study	Jan 2015	0.7	Upper oxic waters	BDL – 0.52[††††]	Niskin	BRM	0.3 GF75	1.2	10	Mean=0.0054 ±0.0026 atom-% (3σ, *n*=7 12.5 μg N standards)	Yes[‡‡‡‡]
			ODZ (~100–700 m)	BDL – 0.77[††††]	Pump[‡‡]	BRM		4.3			Yes[§§§§]
			Below ODZ	BDL	Niskin[‡‡]	BRM		4.3			Yes[‡‡‡‡]

*Geographic distribution of studies displayed in Fig. 3.
[†]Oceanic Niño Index (https://origin.cpc.ncep.noaa.gov/products/analysis_monitoring/ensostuff/ONI_v5.php) is the three-month running mean (period leading up to and including given cruise) sea surface temperature anomaly (based on 30 year mean within area from 5°N to 5°S and 120°W to 170°W). Positive (> 0.5) and negative (< –0.5) values indicate El Niño and La Niña events, respectively.
[‡]"BDL" indicates values that are below the reported detection limit.
[§]TBM, BRM, and ESM refer to the traditional bubble method, the bubble removal method, and the enriched seawater method, respectively. *See* White et al. (2020) for detailed descriptions and comparison.
[¶]$A_{PN_{t=0}}$ refers to ^{15}N-PN atom-% enrichment.
**Care taken to avoid O_2 contamination in low-O_2 samples by filling evacuated gas-tight bags.
[††]In order to achieve a minimum mass of 10 μg N (a reasonable minimum for most instruments; White et al. 2020), ambient PN concentration would need to be > 0.36 μM given a filtration volume of 2 L (as reported by the authors). While mean PN concentrations in the region within the upper 400 m typically exceed this threshold, lower values are often observed, particularly away from coastal upwelling and < ~150 m (Chang et al. 2019; this study; Knapp et al. 2016).
[‡‡]Care taken to avoid O_2 contamination in low-O_2 samples by flushing and filling bottles from the bottom.
[§§]Bottles shaken after $^{15}N_2$ addition to increase rate of gas dissolution.
[¶¶]IRMS linearity verified via Fisher test ($p < 0.01$).
***$A_{PN_{t=0}}$ assumed to be in equilibrium with atmospheric N_2 (0.3663 atom-%).
[†††]Authors reported that most samples exceeded 10 μg N.
[‡‡‡]Values reported here are volumetric rates averaged per station; these values were calculated by dividing reported areal rates (μmol N m^{-2} d^{-1}) for each station by the integration depth.
[§§§]Authors reported "reproducibility" (σ) as equal to 0.0001 atom-%.
[¶¶¶]The mean ^{15}N-PN enrichment in the upper water column was used as $A_{PN_{t=0}}$ for N_2 fixation rate calculations.
****Enriched seawater collected from the same depth and location as sample water.
[††††]If a limit of quantification (10σ, *n* = 7 12.5 μg standards) is applied, then all detectable rates would be considered too low to quantify (< 0.4–1.4 nmol N L^{-1} d^{-1}).
[‡‡‡‡]Mean ^{15}N-PN enrichment within oxic waters was used as $A_{PN_{t=0}}$ when direct measurement was not available (e.g., when mass of collected sample was insufficient).
[§§§§]Mean ^{15}N-PN enrichment within suboxic (< 20 μmol kg^{-1}) waters used as $A_{PN_{t=0}}$ when direct measurement was not available (e.g., when mass of collected sample was insufficient).

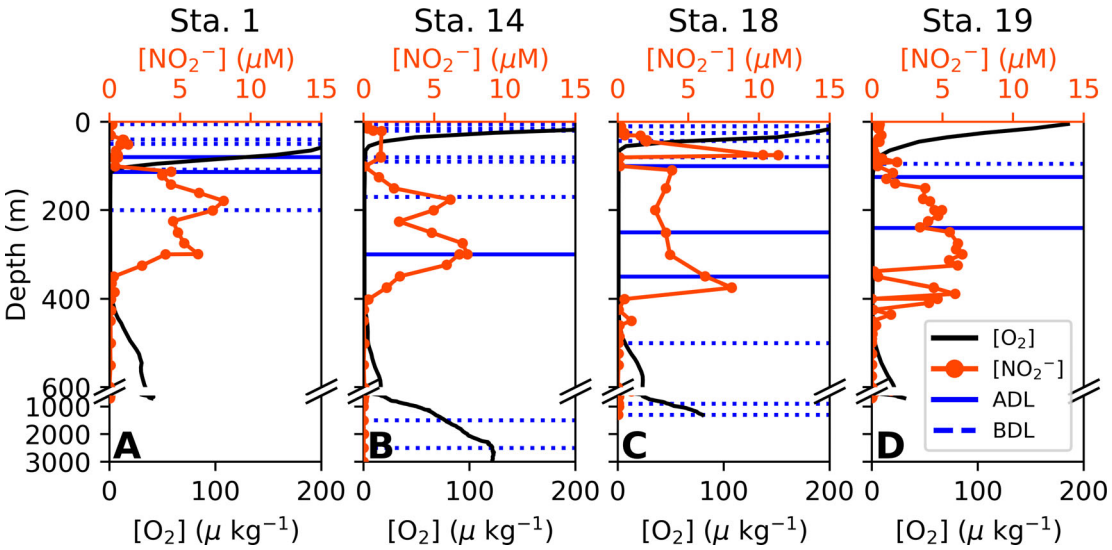

Fig. 2. Sites at which N_2 fixation was detected. Solid and dashed blue lines indicate the depths at which N_2 fixation rates were above (ADL) and below the detection limit (BDL), respectively. Nitrite (NO_2^-; red line) and dissolved oxygen (O_2; black line) profiles indicate the extent of the O_2 deficient zone at each station.

eighth and final detectable rate occurred along a shallow oxycline (Sta. 1, 80 m). Our observation that N_2 fixation is restricted to the upper oxycline/O_2 deficient zone is consistent with prior reporting of a broad N_2 fixation rate peak (< 0.4 nmol N L^{-1} d^{-1}) across the oxycline and upper O_2 deficient zone at nearshore stations (Löscher et al. 2014). Similarly, Chang et al. (2019) observed an increase in *nifH* (a requisite gene for N_2 fixation) concentrations within the O_2 deficient zone, and Löscher et al. (2014) noted that the majority of the *nifH* sequences that they recovered were from within low O_2 waters.

Theoretical calculations suggest that N_2 fixation may offer a slight energetic advantage over NO_3^- assimilation in low O_2 waters where the cost of shielding nitrogenase from oxidative damage is minimized, provided that the organism is capable of recycling electrons (via an uptake hydrogenase) and efficient respiration (Großkopf and LaRoche 2012). Additionally, it has been proposed that some microbes may use nitrogenase as an electron sink as a mechanism for balancing intracellular redox state (e.g., Bombar et al. 2016). These claims are supported by experimental work with Baltic Sea proteobacteria (Bentzon-Tilia et al. 2015). Bentzon-Tilia et al. (2015) observed that all of their isolates increased N_2 fixation at low O_2 concentrations (~ 4–40 μM). Moreover, one isolate, an α-proteobacterium (*Rhodopseudomonas palustris*) closely related to sequences found near our study site (Chang et al. 2019), enhanced its diazotrophic activity upon the addition of ammonium (a reduced N_r compound).

While the observed distribution of detectable N_2 fixation rates reported here supports the idea that low O_2 concentrations may favor diazotrophy, the limited range and low rates observed suggest that diazotrophs active in the Eastern Tropical South Pacific O_2 deficient zone are unlikely to represent a significant source of N_r locally.

The role of organic carbon availability

Most detectable N_2 fixation rates, and all observed within suboxic waters, occurred at stations where coastal upwelling (Fig. 1A) drove high productivity, as indicated by surface chlorophyll *a* concentrations (Fig. 1B). At Sta. 14 and 19, depth-integrated chlorophyll *a* concentrations exceed 100 mg m^{-2} in the euphotic zone—approximately double the average value observed among all stations. Particulate carbon concentrations, indicative of microbial abundance, tended to be high where N_2 fixation was detectable relative to measurements within the O_2 deficient zone at other stations (Suppl. Fig. 3). However, this difference was not statistically significant (Wilcoxon Rank Sum, $n_1 = 8$, $n_2 = 40$, $U = -1.69$, $p = 0.092$).

Several lines of evidence suggest that diazotrophic activity in deep waters is subject to variability in labile organic carbon inputs (which occurs mainly via photosynthetic production in surface waters). (1) Within the Eastern Tropical South Pacific O_2 deficient zone, *nifH* genes/transcripts largely group with proteobacterial sequences, particularly those associated with methylotrophic and heterotrophic bacteria (e.g., Löscher et al. 2014; Turk-Kubo et al. 2014; Chang et al. 2019), including known sulfate-reducers (Bonnet et al. 2013). However, recent work has demonstrated that many marine microbes are more metabolically flexible than previously thought (e.g., Füssel et al. 2017). Thus, diazotrophs that are known heterotrophs may be capable of utilizing different energy acquisition strategies. (2) Direct addition of organic carbon substrates to incubation bottles frequently enhances N_2 fixation rates in O_2 depleted waters (e.g., Bonnet et al. 2013; Löscher

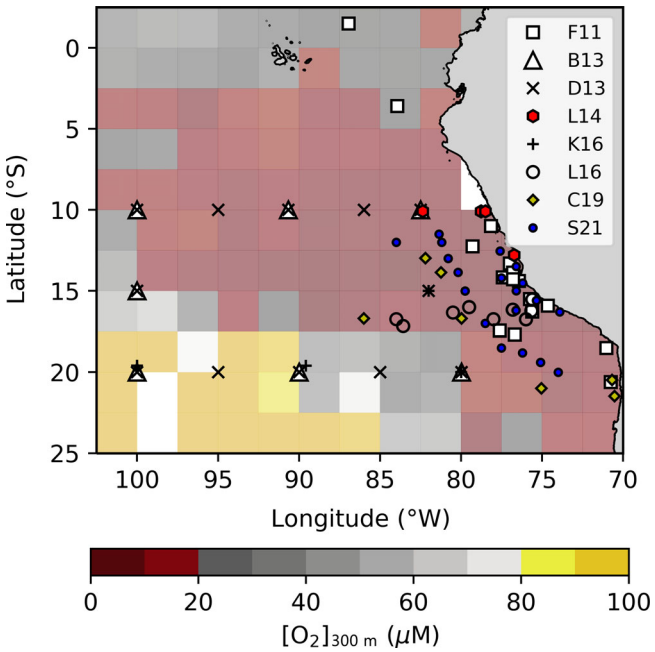

Fig. 3. Sites where N_2 fixation rates have been measured overlying World Ocean Atlas mean dissolved oxygen concentration ($[O_2]$) at 300 m (Garcia et al. 2018), binned per 2.5°. F11 = Fernandez et al. 2011; B13 = Bonnet et al. 2013; D13 = Dekaezemacker et al. 2013; L14 = Löscher et al. 2014; K16 = Knapp et al. 2016; L16 = Löscher et al. 2016; C19 = Chang et al. 2019; S21 = this study.

et al. 2014; Selden et al. 2019). However, these studies have generally observed significant variability in diazotrophic response at different sites and with different substrates. This variability could result from metabolic diversity, including differing substrate preferences, among distinct assemblages. Thus, though imprudent to assume that all diazotrophic activity depends upon organic carbon availability, it may frequently be a relevant factor and may partially explain the distribution of detectable N_2 fixation rates reported here.

Temporal variability

Surface productivity in the Eastern Tropical South Pacific is strongly influenced by upwelling-driven nutrient supply (Pennington et al. 2006). Both seasonal and interannual variability affecting upwelling (e.g., the El Niño-Southern Oscillation) can thus alter the availability of organic substrates above and within the O_2 deficient zone (Pennington et al. 2006). Moreover, benthic Fe supply, likely the major source of Fe both on- and offshore (Cutter et al. 2018), is diminished during periods when upwelling is relaxed and upwelled waters are less reducing (Rapp et al. 2020). As N_2 fixation in the Eastern Tropical South Pacific is thought to be largely Fe-limited (e.g., Dekaezemacker et al. 2013), changes in the Fe inventory may directly affect diazotrophs. Thus, discrepancies among regional studies of N_2 fixation (Table 1) may be partly explained by temporal variability, though we note that methodological differences among studies complicate their comparison (*see* discussion below).

Surface productivity tends to be lower during austral winter than summer, and during El Niño periods (Pennington et al. 2006). N_2 fixation within the O_2 deficient zone has largely been detected in studies conducted during austral summer (Table 1) while the only winter survey (Chang et al. 2019), whose experimental design was most similar to that employed here, failed to detect N_2 fixation below the euphotic zone. With regard to interannual variability, N_2 fixation rates within the O_2 deficient zone vary more among individuals studies than between El Niño (Bonnet et al. 2013; Fernandez et al. 2011; this study) and La Niña periods (Bonnet et al. 2013; Löscher et al. 2014), or periods of mean condition (Fernandez et al. 2011; Löscher et al. 2016; Chang et al. 2019). This likely reflects the degree to which methodological choices influence the detection and calculation of low rates (*see* discussion below), at least in part. However, spatial heterogeneity in the effects of El Niño/La Niña (e.g., Rapp et al. 2020) may help explain discrepancies among these studies as well, given their far-ranging distribution—from the continental shelf to the edge of the South Pacific gyre (Fig. 3).

Rapp et al. (2020) observed that Fe concentrations were significantly reduced during the 2015–2016 El Niño event (concurrent with this study) along onshore-offshore transects crossing the Peruvian continental shelf, except where the shelf was thinnest (corresponding to Sta. 18 in this study). Here, Fe concentrations were on par with those previously reported during La Niña events and neutral conditions. We observed detectable N_2 fixation at two nearshore stations along this narrow portion of the shelf (Sta. 18 and 19; Fig. 1), representing five of the eight detectable rates (of 125 measurements) observed in this study. This suggests that Fe availability was an important factor regulating our observed distribution of N_2 fixation. Indeed, the highest N_2 fixation rate recorded in the region was observed during La Niña at a nearshore station (between Sta. 12 and 13 in this study) where the sulfide/NO_2^- transition was remarkably shallow (~ 30 m) and dissolved Fe concentrations exceeded 150 nmol kg^{-1} at the surface (Löscher et al. 2014). Local N_2 fixation may thus be closely coupled to temporal variability affecting Fe cycling.

Interpretation of low rates

Overestimation

The potential for low N_2 fixation rates in deep, subeuphotic environments (Moisander et al. 2017; Benavides et al. 2018) has instigated reconsideration of how to apply the $^{15}N_2$ tracer assay in pelagic environments (White et al. 2020). N_2 fixation rate methodology in the Eastern Tropical South Pacific O_2 deficient zone has therefore varied (Table 1), complicating comparisons between studies. Rates may be overestimated when the natural abundance of ^{15}N in the PN pool (i.e., $A_{PN_{t=0}}$) is assumed rather than measured, when the mass of PN on the filter is too low (e.g., < 10 μg N), and/or detection

limits are not calculated based on instrument performance (*see* White et al. 2020 for comprehensive discussion).

Some studies assume that $A_{PN_{t=0}}$ is in equilibrium with atmospheric N_2 (0.3663 atom-%). This is a poor assumption within and around denitrified waters and in many environments where the dissolved N_r pool is highly dynamic; we observed a mean $A_{PN_{t=0}}$ of 0.3692 ± 0.0018 atom-% (n = 146) throughout all surveyed waters at the time of our study. The difference between these values would have constituted detectable enrichment in about one-third of our IRMS runs in this study. Moreover, the mean natural abundance of ^{15}N in PN is typically greater in suboxic waters than in the overlying waters (Chang et al. 2019; this study; Voss et al. 2001). Consequently, the use of surface $A_{PN_{t=0}}$ measurements for incubations conducted with suboxic water may result in the overestimation of rates from deeper waters. In January 2015, $A_{PN_{t=0}}$ was significantly different between suboxic (0.3700 ± 0.0016 atom-%, n = 44) and oxic waters (0.3690 ± 0.0017 atom-%, n = 94; one-way ANOVA, df = 136, F = 11.85, p = 0.0002 based on 10,000 random permutations). These values are consistent with those reported by Chang et al. (2019) in July 2011, suggesting low seasonal/interannual variability.

The mass of PN collected on the filter at the end of the incubation is also crucial for accurate instrument detection. When sample mass is too low, typically below ~ 10 μg N, isotope ratio measurements often drift (Suppl. Fig. 1; White et al. 2020). Either positive drift in $A_{PN_{t=f}}$ or negative drift in $A_{PN_{t=0}}$ may falsely inflate N_2 fixation rates. Even when mass is sufficiently high, analytical variability may affect the relative difference between $A_{PN_{t=0}}$ and $A_{PN_{t=f}}$, necessitating the determination of a minimum detectable difference in A_{PN} based on instrument variability (e.g., 3σ of standards) from which a detection limit can be calculated (White et al. 2020). As variability is a function of mass (Suppl. Fig. 1; White et al. 2020), a conservative minimum detectable difference would be one based on the variability of standards at the lower end of the sample mass range. Where reported, minimum detectable differences in enrichment for Eastern Tropical South Pacific studies vary by ~ 10× (Table 1). We note that calculating N_2 fixation rate uncertainty as the standard deviation of rates from replicate incubations does not constrain variability in $A_{PN_{t=0}}$, complicating inter-comparisons of low rates (Suppl. Text 1).

Underestimation

N_2 fixation rates may be underestimated because of slow $^{15}N_2$ equilibration (Mohr et al. 2010) when employing the traditional bubble method (Montoya et al. 1996), inappropriately large filter pore-size in systems with small diazotrophs (Bombar et al. 2018), drift in A_{PN} measurements at low mass (*see* above), and/or inhibition of low O_2-adapted organisms by O_2 contamination during sampling. Löscher et al. (2014) found that O_2 exposure (10 μM) in low O_2 incubations reduced the abundance of *nifH* associated with some non-cyanobacterial diazotrophs. While O_2 exposure is minimized by collecting samples using a submersible pump (as deployed in this study), even minor shifts in O_2 and substrate availability, temperature and pressure can alter the activity of O_2 deficient zone microbial communities (Stewart et al. 2012). Most studies from the Eastern Tropical South Pacific have attempted to address the issue of O_2 contamination (Table 1); however, the efficacy of different approaches and the effect of O_2 intrusion on N_2 fixation rates in suboxic waters, has not been assessed.

Summary

Given the issues outlined here, we proffer that some previous studies in the Eastern Tropical South Pacific may have overestimated N_2 fixation rates there. Depth-integration of rates near the analytical detection limit can compound this issue, making it essential that error is accurately calculated and propagated (Suppl. Text 1). Such overestimation of measured rates could resolve the discrepancy observed in the Eastern Tropical South Pacific between previously reported values and those predicted from the abundance of dominant proteobacterial diazotroph groups (Turk-Kubo et al. 2014).

In addition to the methodological differences outlined above (Table 1), discrepancies among N_2 fixation rates in surface waters between this and previous studies may also be attributable to temporal (*see* discussion above) and geographic differences among these studies; Bonnet et al. (2013), Dekaezemacker et al. (2013) and Knapp et al. (2016) all focused on the periphery of the South Pacific Subtropical Gyre, further offshore than this study (Fig. 3). However, given that sub-euphotic diazotrophs typically respond to organic matter inputs suggestive of heterotrophic carbon limitation (e.g., Bonnet et al. 2013; Löscher et al. 2014), we consider it unlikely that sub-euphotic N_2 fixation rates would be higher further offshore than beneath relatively more productive upwelling waters. Ultimately, differentiating detectable and undetectable N_2 fixation rates with sensitivity has far-ranging implications for our understanding of oceanic N budgets and N_2 fixation in marine systems.

Conclusions

Our conservative evaluation contradicts previous reports of low but persistent N_2 fixation rates throughout the Eastern Tropical South Pacific O_2 deficient zone (Table 1), which are often cited in support of the hypothesis that N_2 fixation is widespread in the ocean's interior (e.g., Benavides et al. 2018). Instead, our work suggests that N_2 fixation in this region is sparse and restricted to low O_2 waters in the upper O_2 deficient zone. Our findings support the idea that low O_2 conditions (e.g., Großkopf and LaRoche 2012; Bombar et al. 2016) and high surface productivity (e.g., Löscher et al. 2014) may favor N_2 fixation by non-cyanobacterial diazotrophs despite significant concentrations of ambient DIN. However, N_2

fixation in the Eastern Tropical South Pacific does not appear to be a quantitatively important source of N_r either locally or globally. Quantifying the contribution of deep waters, where metabolic rates are low, to global biogeochemical cycles will ultimately require more sensitive discernment of biological signals from noise as we push the boundaries of analytical detection.

Data availability statement

Data presented here are available in the Supporting Material as well as on BCO-DMO (http://www.bco-dmo.org/project/742492).

References

Benavides, M., S. Bonnet, I. Berman-Frank, and L. Riemann. 2018. Deep into oceanic N_2 fixation. Front. Mar. Sci. **5**: 108. doi:10.3389/fmars.2018.00108

Bentzon-Tilia, M., I. Severin, L. H. Hansen, and L. Riemann. 2015. Genomics and ecophysiology of heterotrophic nitrogen-fixing bacteria isolated from estuarine surface water. mBio **6**: e00929–e00915. doi:10.1128/mBio.00929-15

Bombar, D., R. W. Paerl, and L. Riemann. 2016. Marine non-cyanobacterial diazotrophs: Moving beyond molecular detection. Trends Microbiol. **24**: 916–927. doi:10.1016/j.tim.2016.07.002

Bombar, D., R. W. Paerl, R. Anderson, and L. Riemann. 2018. Filtration via conventional glass fiber filters in $^{15}N_2$ tracer assays fails to capture all nitrogen-fixing prokaryotes. Front. Mar. Sci. **5**: 6. doi:10.3389/fmars.2018.00006

Bonnet, S., et al. 2013. Aphotic N_2 fixation in the eastern tropical South Pacific Ocean. PLoS One **8**: e81265. doi:10.1371/journal.pone.0081265

Bonnet, S., M. Caffin, H. Berthelot, and T. Moutin. 2017. Hot spot of N_2 fixation in the western tropical South Pacific pleads for a spatial decoupling between N_2 fixation and denitrification. PNAS **114**: E2800–E2801. doi:10.1073/pnas.1619514114

Chang, B. X., and others. 2019. Low rates of dinitrogen fixation in the eastern tropical South Pacific. Limnol. Oceanogr. **64**: 1913–1923. doi:10.1002/lno.11159

Cutter, G. A., J. W. Moffett, M. C. Nielsdóttir, and V. Sanial. 2018. Multiple oxidation state trace elements in suboxic waters off Peru: In situ redox processes and advective/diffusive horizontal transport. Mar. Chem. **201**: 77–89. doi:10.1016/j.marchem.2018.01.003

Dabundo, R., and others. 2014. The contamination of commercial $^{15}N_2$ gas stocks with ^{15}N-labeled nitrate and ammonium and consequences for nitrogen fixation measurements. PLoS One **9**: e110335. doi:10.6084/m9.figshare.1170194

Dekaezemacker, J., S. Bonnet, O. Grosso, T. Moutin, M. Bressac, and D. Capone. 2013. Evidence of active dinitrogen fixation in surface waters of the eastern tropical South Pacific during El Niño and La Niña events and evaluation of its potential nutrient controls. Global Biogeochem. Cycles **27**: 768–779. doi:10.1002/gbc.20063

Deutsch, C., D. M. Sigman, R. C. Thunell, A. N. Meckler, and G. H. Haug. 2004. Isotopic constraints on glacial/interglacial changes in the oceanic nitrogen budget. Global Biogeochem. Cycles **18**: GB4012. doi:10.1029/2003GB002189

Deutsch, C., J. L. Sarmiento, D. M. Sigman, N. Gruber, and J. P. Dunne. 2007. Spatial coupling of nitrogen inputs and losses in the ocean. Nature **445**: 163–167. doi:10.1038/nature05392

Devol, A. 2008. Denitrification including anammox, p. 263–301. *In* D. G. Capone, D. A. Bronk, M. R. Mulholland, and E. J. Carpenter [eds.], Nitrogen in the marine environment. Academic Press.

DeVries, T., C. Deutsch, F. Primeau, B. Chang, and A. Devol. 2012. Global rates of water-column denitrification derived from nitrogen gas measurements. Nat. Geosci. **5**: 547–550. doi:10.1038/ngeo1515

Falkowski, P. G. 1983. Enzymology of nitrogen assimilation, p. 839–868. *In* D. G. Capone and E. J. Carpenter [eds.], Nitrogen in the marine environment. Elsevier.

Falkowski. 1997. Evolution of the nitrogen cycle and its influence on the biological sequestration of CO_2 in the ocean. Nature **387**: 272–275. doi:10.1038/387272a0

Fernandez, C., L. Farías, and O. Ulloa. 2011. Nitrogen fixation in denitrified marine waters. PLoS One **6**: e20539. doi:10.1371/journal.pone.0020539

Füssel, J., and others. 2017. Adaptability as the key to success for the ubiquitous marine nitrite oxidizer Nitrococcus. Sci. Adv. **3**: e1700807. doi:10.1126/sciadv.1700807

Garcia, H., and others. 2018. World Ocean Atlas 2018 Vol. 3: Dissolved oxygen. Apparent oxygen utilization, and dissolved oxygen saturation. NOAA Atlas NESDIS 83.

Großkopf, T., and J. LaRoche. 2012. Direct and indirect costs of dinitrogen fixation in *Crocosphaera watsonii* WH8501 and possible implications for the nitrogen cycle. Front. Microbiol. **3**: 236. doi:10.3389/fmicb.2012.0023

Jayakumar, A., B. X. Chang, B. Widner, P. Bernhardt, M. R. Mulholland, and B. B. Ward. 2017. Biological nitrogen fixation in the oxygen-minimum region of the eastern tropical North Pacific Ocean. ISME J. **11**: 2356–2367. doi:10.1038/ismej.2017.97

Karl, D., and others. 2002. Dinitrogen fixation in the world's oceans, p. 47–98. *In* The nitrogen cycle at regional to global scales. Springer.

Knapp, A. N., K. L. Casciotti, W. M. Berelson, M. G. Prokopenko, and D. G. Capone. 2016. Low rates of nitrogen fixation in eastern tropical South Pacific surface waters. PNAS **113**: 4398–4403. doi:10.1073/pnas.1515641113

Knapp, A., K. Mccabe, O. Grosso, N. Leblond, T. Moutin, and S. Bonnet. 2018. Distribution and rates of nitrogen fixation in the western tropical South Pacific Ocean constrained by

nitrogen isotope budgets. Biogeoscience **15**: 2619–2628. doi:10.5194/bg-15-2619-2018

Kondo, Y., and J. W. Moffett. 2015. Iron redox cycling and subsurface offshore transport in the eastern tropical South Pacific oxygen minimum zone. Mar. Chem. **168**: 95–103. doi:10.1016/j.marchem.2014.11.007

Löscher, C. R., and others. 2014. Facets of diazotrophy in the oxygen minimum zone waters off Peru. ISME J. **8**: 2180–2192. doi:10.1038/ismej.2014.71

Löscher, C. R., and others. 2016. N_2 fixation in eddies of the eastern tropical South Pacific Ocean. Biogeoscience **13**: 2889–2899. doi:10.5194/bg-13-2889-2016

Mohr, W., T. Grosskopf, D. W. Wallace, and J. LaRoche. 2010. Methodological underestimation of oceanic nitrogen fixation rates. PLoS One **5**: e12583. doi:10.1371/journal.pone.0012583

Moisander, P. H., M. Benavides, S. Bonnet, I. Berman-Frank, A. E. White, and L. Riemann. 2017. Chasing after non-cyanobacterial nitrogen fixation in marine pelagic environments. Front. Microbiol. **8**: 1736. doi:10.3389/fmicb.2017.01736

Montoya, J. P., M. Voss, P. Kahler, and D. G. Capone. 1996. A simple, high-precision, high-sensitivity tracer assay for N_2 fixation. Appl. Environ. Microbiol. **62**: 986–993.

Moore, C., and others. 2013. Processes and patterns of oceanic nutrient limitation. Nat. Geosci. **6**: 701–636. doi:10.1038/NGEO3006

NASA Goddard Space Flight Center, O. B. P. G. Reprocessing. 2018. Moderate-resolution imaging spectroradiometer (MODIS) aqua chlorophyll data. NASA Ocean Biology Distibuted Active Archive Center (OB.DAAC), Goddard Space Flight Center, Greenbelt, MD.

Pai, S. C., C. C. Yang, and J. P. Riley. 1990. Formation kinetics of the pink azo dye in the determination of nitrite in natural waters. Anal. Chim. Acta **232**: 345–349. doi:10.1016/S0003-2670(00)81252-0

Parsons, T. R., Y. Maita, and C. M. Lalli. 1984. A manual of biological and chemical methods for seawater analysis. Publ. Pergamon Press.

Pennington, J. T., K. L. Mahoney, V. S. Kuwahara, D. D. Kolber, R. Calienes, and F. P. Chavez. 2006. Primary production in the eastern tropical Pacific: A review. Prog. Oceaongr. **69**: 285–317. doi:10.1016/j.pocean.2006.03.012

Rapp, I., and others. 2020. El Niño-driven oxygenation impacts Peruvian shelf iron supply to the South Pacific Ocean. Geophys. Res. Lett. **47**: e2019GL086631. doi:10.1029/2019GL086631

Ripp, J. 1996. Analytical detection limit guidance & laboratory guide for determining method detection limits. Wisconsin Department of Natural Resources, Laboratory Certification Program.

Selden, C., M. Mulholland, P. Bernhardt, B. Widner, A. Macías-Tapia, J. Qi, and A. Jayakumar. 2019. Dinitrogen fixation across physico-chemical gradients of the eastern tropical North Pacific oxygen deficient zone. Global Biogeochem. Cycles **33**: 1187–1202. doi:10.1029/2019GB006242

Stewart, F. J., and others. 2012. Experimental incubations elicit profound changes in community transcription in OMZ bacterioplankton. PLoS One **7**: e37118. doi:10.1038/ismej.2010.18

Thamdrup, B., T. Dalsgaard, and N. P. Revsbech. 2012. Widespread functional anoxia in the oxygen minimum zone of the eastern South Pacific. Deep-Sea Res.: Part I **65**: 36–45. doi:10.1016/j.dsr.2012.03.001

Turk-Kubo, K. A., M. Karamchandani, D. G. Capone, and J. P. Zehr. 2014. The paradox of marine heterotrophic nitrogen fixation: Abundances of heterotrophic diazotrophs do not account for nitrogen fixation rates in the eastern tropical South Pacific. Environ. Microbiol. **16**: 3095–3114. doi:10.1111/1462-2920.12346

Voss, M., J. W. Dippner, and J. P. Montoya. 2001. Nitrogen isotope patterns in the oxygen-deficient waters of the eastern tropical North Pacific Ocean. Deep-Sea Res.: Part I **48**: 1905–1921. doi:10.1016/S0967-0637(00)00110-2

Weber, T., and C. Deutsch. 2014. Local versus basin-scale limitation of marine nitrogen fixation. PNAS **111**: 8741–8746. doi:10.1073/pnas.1317193111

White, A. E., et al. 2020. A critical review of the $^{15}N_2$ tracer method to measure diazotrophic production in pelagic ecosystems. Limnol. Oceanogr.: Methods **18**: 129–147. doi:10.1002/lom3.10353

Zehr, J. P., and D. G. Capone. 2020. Changing perspectives in marine nitrogen fixation. Science **368**: eaay9514. doi:10.1126/science.aay9514

Acknowledgments

We thank the captain and crew of the R/V *Atlantis*, the scientists who participated in sample collection and analysis, particularly Shannon Cofield and Steve Stone, and Bess Ward for the use of her facilities at Princeton University. We also thank Bonnie Chang for her role in cruise planning and execution as well as sample collection and analysis of the $^{15}N_2$ samples. Finally, we thank Osvaldo Ulloa and Gadiel Alarcón for contributing and operating the pump profiling system, respectively. This work was funded by the National Science Foundation Division of Ocean Sciences (NSF-OCE) Grant OCE-1356056 to M.R.M. and A.J.

Conflict of Interest

None declared.

Submitted 19 September 2020
Revised 19 December 2020
Accepted 21 February 2021

Associate editor: Ilana Berman-Frank